Catalysis Science & Technology

Accepted Manuscript

ROYAL SOCIETY OF CHEMISTRY

www.rsc.org/catalysis

Transesterification of soybean oil (SBO) with methanol at 100°C		
Catalyst	SBO Conversion (%)	FAME Yield (%)
Zn-Ac	94.4	63.1
Zn-Nit	83.9	51.5

Journal Name

ARTICLE

Synthesis of Biodiesel from Soybean Oil Using Zinc Layered Hydroxide Salts as Heterogeneous Catalysts

D.M. Reinoso, D.E. Damiani, G.M. Tonetto[*]

In this work, the transesterification of soybean oil with methanol using layered heterogeneous catalysts to produce biodiesel was studied. The zinc hydroxy acetate salt $Zn_5(OH)_8(CH_3COO)_2.4H_2O$ (abbreviated Zn-Ac) and zinc hydroxy nitrate $Zn_5(OH)_8(NO_3)_2.2H_2O$ (abbreviated Zn-Nit), which have a layered structure, were synthesized (chemical precipitation) and characterized by X-ray diffraction, infrared spectroscopy, scanning electron microscopy, particle size distribution measurements, specific surface area determination and thermogravimetric analysis. Zn-Ac and Zn-Nit were tested in the transesterification of soybean oil at 100 °C for 2 h. Zn-Nit presented 83.9% oil conversion with 51.5% FAME yield, and it was stable in three consecutive tests, also showing good tolerance to aqueous content. Zn-Ac was not stable. The salts transformed into Zn glycerolate at 140 °C in the reaction medium.

A. Introduction

In recent years there has been an increasing demand for biodiesel, consisting of methyl or ethyl esters of fatty acids, as a substitute for conventional petroleum-derived diesel because its renewable nature is effective in easing down greenhouse gas emissions.[1] Additionally, biodiesel is superior to fossil diesel fuel in terms of cetane number, flash point and lubricity characteristics, which prolongs engine life.

The methyl or ethyl esters of fatty acids can be produced by the transesterification of vegetable oils and animal fats with low molecular weight alcohols.

Biodiesel was generally manufactured by a process using a homogeneous base catalyst such as sodium and potassium methoxides and hydroxides. Industrially, NaOH and KOH are preferred due to their wide availability and low cost. Base catalysts are preferred to acid catalysts because they are more active.[2] However, these homogeneous catalytic systems have many disadvantages. Removal of these catalysts to purify the biodiesel fuel and glycerol as a by-product is difficult and requires large amounts of water. Consequently, a considerable amount of waste water is inevitably produced.

Transesterification over efficient heterogeneous catalysts is a promising route that enables to overcome these problems. Solid catalysts can be easily separated from reactants by filtration and facilitate the use of continuously operated reactors such as fixed-bed reactors. For this reason, stability is an important property in solid catalysts for the synthesis of biodiesel, where leaching of the active species should be avoided. If the leaching phenomenon is important, the species act as a homogeneous catalyst and the solid is gradually deactivated.

There are reports on the heterogeneous catalytic transesterification of highly refined oils, acid and crude oils. A great variety of heterogeneous base catalysts have been investigated, including pure oxides and hydroxides of alkaline earth metals such as MgO,[3] CaO,[4] SrO,[5] and BaO[6] as well as promoted and supported catalysts comprising these oxides.[7,8] Also zeolites, hydrotalcites[9,10,11,12,13,14,15,16] and other oxides[15] have been studied.

Some works related to the use of base Zn compounds in transesterification and esterification reactions have been reported in the literature. This metal can act as a Lewis acid center (Zn^{2+}),[17,18] or it can be part of solid base compounds. In the first case, an interaction of the carbonyl oxygen of the triglyceride with the Lewis acidic site of the catalyst occurs, forming a carbocation, followed by the nucleophilic attack by the alcohol.[19] The second case involves the activation of an alcohol as a nucleophilic reactant to attack the electrophilic carbon of carboxylate esters.[20]

Focusing on the second group, we can mention ZnO, which is a weak base. Suppes et al.[15] reported that zinc oxide was moderately active in the transesterification reaction. Zinc oxide doped with alkali and alkaline earth metals showed to be an effective heterogeneous base catalyst for soybean oil transesterification.[21,22] Recently, good results were obtained for the mixture of CaO and ZnO oxides with high activity and satisfactory stability.[23,24]

Zinc aluminates, stoichiometric or having an excess of Zn, are base materials.[25,26] ZnAl mixed oxides were studied in the base-catalyzed transesterification process for biodiesel production, although an acid cooperation occurs with this type of catalysts. Jiang et al.[27] tested Zn-Al complex oxide catalysts with a hydrotalcite-like structure in the transesterification of rapeseed oil, with high conversion. Montanari et al.[28] synthesized a Zn-Al mixed oxide with very weak Lewis acid sites and high basicity which originated methanol adsorption and gave rise to the formation of terminal alcoholate species characterized by a strong ionicity.

One of the catalysts that exhibited good activity under moderate reaction conditions was zinc hydroxy nitrate $(Zn_5(OH)_8(NO_3)_2.2H_2O)$, a base solid which belongs to the class of

layered hydroxide salts.[29,30] This catalyst showed to be an active heterogeneous catalyst, without any leaching, in the transesterification of triglycerides with methanol, and it retained its activity in subsequent catalytic cycles. However, it was also reported that during esterification of fatty acids, the layered solid gradually decomposed losing its structure.[31] It was also found that when the salt was treated at temperatures above 105 °C, it started to decompose, and its activity in transesterification in subsequent reuses begun to decrease.[32]

Zinc hydroxy nitrate presents a layered structure consisting of infinite brucite-like layers, where one quarter of the octahedrally coordinated Zn atom sites are vacant, and on either side of the empty octahedra there are zinc atoms tetrahedrally coordinated to OH groups (forming the base of the tetrahedra) with a water molecule occupying the apex. The nitrate groups are located between the sheets, and they are not involved in the coordination of the Zn atoms.[33]

Zinc hydroxy acetate $Zn_5(OH)_8(CH_3CO_2)_2.4H_2O$ is a similar layered salt, but it presents a larger separation between layers.[34] The mode of interaction between the acetate anion and the matrix cation is not yet clear. It was proposed that the anion occurs as a free species,[35,36] while in a recent report it was hypothesized that the acetate anion is directly coordinated to the matrix cation as a unidentate ligand via M–OCOCH$_3$ bonds.[37]

In the present work, zinc hydroxy acetate and zinc hydroxy nitrate salts were compared for the transesterification reaction of soybean oil at 100 and 140 °C, and the efficiency of the catalysts was evaluated in terms of conversion of soybean oil and fatty acid methyl ester (FAME) yield. The stability of the catalysts was carefully analyzed, and the effect of water was investigated.

2. Experimental

2.1. Catalyst preparation

The $Zn_5(OH)_8(NO_3)_2.2H_2O$ (Zn-Nit) was synthesized according to the procedure reported by Newman and Jones.[38] The Zn-Nit salt was prepared by addition of 0.75 M sodium hydroxide solution to 3.5 M zinc nitrate aqueous solution at room temperature, with constant stirring.

The $Zn_5(OH)_8(CH_3CO_2)_2.4H_2O$ (Zn-Ac) was prepared according to Biswick et al.[34] The Zn-Ac salt was synthesized by addition of 0.75 M sodium hydroxide solution to 0.7 M zinc acetate dihydrate aqueous solution.

2.2 Catalyst characterization

The samples Zn-Ac and Zn-Nit (synthesized and recovered after reaction) were analyzed by X-ray diffraction (Philips PW1710, using Cu Kα radiation scan) and diffuse-reflectance Fourier transform-infrared spectroscopy (DRIFTS, Nicolet 6700FT-IR spectrometer).

The textural characterization of the solids was obtained from the N_2 adsorption isotherm at 77K (Quantachrome instrument). The surface areas were calculated by BET method and the pore size distribution by the BJH method.

The morphology of the powder catalysts was analyzed by SEM using a JEOL 35 CF scanning electron microscope.

The amount of Zn in the catalysts (before and after the reaction) was determined by atomic adsorption spectrometry (AAS, Perkin Elmer Analyst 700).

The thermogravimetric (TGA) curve of the catalysts was determined using a thermogravimetric analyzer (Perkin Elmer II) under N_2 flow from room temperature to 800 °C (at a heating rate of 20 °C min^{-1}).

The catalyst particle size distribution was evaluated using a Partica LA-950 V2 laser diffraction particle size distribution analyzer (HORIBA).

The basicity of the solids was estimated by the benzoic acid titration method using indicators. A slurry with 100 mg of solid Zn-Ac and Zn-Nit and the indicators (bromothymol blue and phenolphthalein) was titrated with 0.01 M solution of benzoic acid in methanol.[39]

2.3. Catalytic tests

The catalytic tests were carried out in duplicates in a 600 cm^3 Parr reactor (internal diameter: 64 mm) equipped with a 4-angled blade stirrer, operated in batch mode.

Reactions were studied at 100 and 140 ºC, with an agitation rate of 500 rpm and a reaction time of 2 h. The reactants and the catalyst were fed into the reactor and then the system was heated up until reaction temperature was reached. At that moment, the agitation was started and a zero time sample was taken.

Soybean oil (Argentinian commercial brand, with 1.8 10^{-3} wt% of free fatty acid), without any special pretreatment, and methanol (UVE HPLC) were used. The fatty acid methyl esters (FAME) derived from soybean oil, determined by GC method, are shown in Table 1. The methanol/oil molar ratio was 30:1, and the catalyst loading was 3 wt% (with respect to oil).

Additional experiments were conducted in order to quantify the influence of external mass transfer: the catalytic tests were performed at different stirrer rates (from 300 to 1100 rpm). In order to study the reusability of the samples, three consecutive tests were performed at 100 and 140 °C (the solids were washed with hexane and tetrahydrofuran:methanol). The effect of water content on the transesterification reaction was studied by adding 0.5 wt% of water (with respect to oil) into the reaction medium under usual conditions. Reaction samples were centrifuged to improve the separation of methanol from the oil phase. A ~50 mg sample was taken from the oil phase and prepared for chromatographic analysis. The chromatography of the raw materials and products was carried out in a Perkin Elmer AutoSystem XL equipment with a DB-17HT capillary column and a FID detector (according to the standard UNE-EN 14105 norm).

The triglyceride (TG) conversion (X) and FAME yield (Y) were calculated using the following equations:

$$X_{TG} = \frac{molTG_{t0} - molTG_{tf}}{molTG_{t0}} \qquad (1)$$

$$Y_{FAME} = \frac{mol\,FAME_{tf}\,/3}{molTG_{t0}} \qquad (2)$$

Table 1 Composition of fatty acid methyl esters (FAME) derived from soybean oil.

Fatty acid methyl ester components (number of C atoms)	Content (wt.%)
C16:0	11
C18:0	5.2
C18:1	25.7
C18:2	51.3
C18:3	4.9
C20:0	1.3
C22:0	0.5

3. RESULTS AND DISCUSSION

3.1. Synthesized solids

The morphological properties of the synthetized solid catalysts were measured. The specific surface areas were 25 and 28 m^2/g and the pore volume were 7.1×10^{-2} and 5.1×10^{-2} for Zn-Ac and Zn-Nit, respectively.[31] Both samples presented similar morphological properties with a significant difference in the particle size (7.6 and 26.7μm for Zn-Ac and Zn-Nit).

The basicity of the solids Zn-Ac and Zn-Nit was estimated by benzoic acid titration of the base sites in the presence of pH indicator. This technique provides a first indication of the total basicity of the solid.[40] The number of weak base sites (as measured in the titration with bromothymol blue) was 0.14 and 1.2 mmol/g cat for Zn-Nit and Zn-Ac, respectively. The number of strong base sites can be measured with phenolphthalein as indicator. In the case of the solids Zn-Ac and Zn-Nit, the presence of strong base sites was not detected.

It is very important to analyze the range of thermal stability for this family of solids, since they undergo multiple transformations. This analysis will determine the best operable reaction temperature range. TGA and differential thermogravimetric (DTG) curves for the Zn-Ac and Zn-Nit catalysts are shown in Figures 1 and 2, respectively.

In the case of the Zn-Ac catalyst, it was proposed that the thermal degradation of Zn-Ac takes place in two steps.[34,35,36] In the first step, three processes took place involving only the loss of water. Firstly (50-80 °C) there was the dehydration of the layered material to form $Zn_5(OH)_8(CH_3COO)_2$, which took place up to 160 °C, followed by the dehydroxylation of the hydroxide layers, giving the compounds $Zn_3(OH)_4(CH_3COO)_2$ and $Zn(CH_3COO)_2$ and taking place to 160-230°C. The mass loss for these two processes was 25%. Finally, In the second step, between 230 and 350 °C occurs the decomposition of $Zn(CH_3COO)_2$ to give ZnO with a mass loss of approximately 16%..

In the case of the Zn-Nit catalyst, the TGA curve (Fig. 2) shows that the degradation of the Zn-Nit solid started at 80 °C, and it took place up to 160 °C, with a mass loss of 6% corresponding to the dehydration process to give $Zn_5(OH)_8(NO_3)_2$.[32,33,41] Then the material underwent dehydroxylation (160-250 °C), giving $Zn_3(OH)_4(NO_3)_2$ and $Zn(NO_3)_2$, with an additional mass loss of 20%.

The last step of the thermal degradation is observed at 250 °C, until a constant mass value of 65% is reached at 300 °C. This step is associated only with the degradation of the nitrate ions from the $Zn_3(OH)_4(NO_3)_2$ and $Zn(NO_3)_2$ compounds.
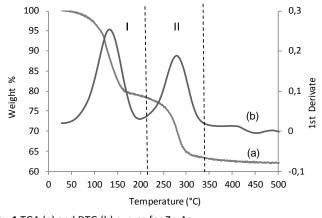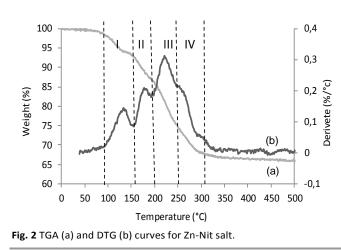

Fig. 2 TGA (a) and DTG (b) curves for Zn-Nit salt.

In summary, the dehydration of the solids was observed from 50-160 °C for Zn-Ac and from 80-160 °C for Zn-Nit. At higher temperatures the material underwent dehydroxylation, giving $Zn_3(OH)_4(CH_3COO)_2$ and $Zn_3(OH)_4(NO_3)_2$. Based on these results, the solids were tested in reaction at 100 and 140 °C (in order to analyze the activity of the dehydrated solids).

An additional thermal treatment was carried out on the layered salts. The synthesized solids were thermally treated for 2 h at 100, 120 and 140 °C in N$_2$ flow (20 cm^3/min). X-ray diffraction patterns and DRIFT spectra of the synthesized Zn-Ac and the thermally treated salts are shown in Figure 3 and 4.

The XRD pattern of Zn-Ac was typical of layered hydroxide salts with preferential orientation in the axial plane 001. The characteristic peaks were located at 2θ = 6.20° (001), 32.89° (100), 12.41° (002), 18.10°(003) and 58.97° (110) and the cell parameters (a=2.72 Å and c=14.39 Å) were compared to published reports.[34,35,36] When the sample was treated at 100 and 120 °C, an important peak was observed at 2θ = 5° with a basal spacing of 17.4 and 17.6 Å, respectively. According to Biswick et al.[34] the resultant species is $Zn_3(OH)_4(CH_3COO)_2$. At 140 °C, the XRD pattern showed ZnO formation (peak at 31.8°, 36.3°, 37.7°, 47.6° and 56.6°)[36,42] and the signals at 2θ = 11.9 and 12.5° are characteristic of zinc acetate (JCPDS card N°00-001-0089) and zinc acetate dihydrate (JCPDS card N° 00-033-1464). Comparing these results with those of the TGA, it can be observed that when the treatment time is increased, dehydroxylation occurs at a lower temperature.
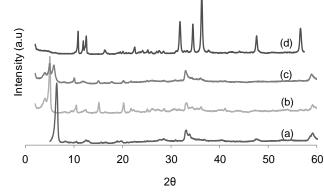

Fig. 3 X-ray diffraction pattern of synthesized Zn-Ac salt (a) and Zn-Ac thermally treated at: (b) 100 °C, (c) 120 °C, (d) 140 °C.

Fig. 1 TGA (a) and DTG (b) curves for Zn-Ac.

In the DRIFT spectra of Zn-Ac (Fig.4.a) and the thermally treated samples (Fig.4.b-d), no major differences were observed. The strong band observed at 3673 cm^{-1} can be attributed to stretching vibrations of OH groups not involved in hydrogen bonding, and the broad band at 3450 cm^{-1} can be ascribed to OH groups involved in hydrogen bonding. The signal at 3600 decreased with increasing temperature. The sharp absorption bands at 1585, 1391 and 2900 cm^{-1} can be ascribed to the vibrations of the carboxylic group from the acetate anion. The bands at 1338 and 1021 cm^{-1} are attributed to the deformation of CH$_3$ groups and the vibrations of the OH group, respectively.[33,35,43]

It can be highlighted that DRIFT results for Zn-Ac showed that the basic functional groups were still present in all the solids, nevertheless the XRD patterns showed very different structures as a consequence of the thermal treatment.
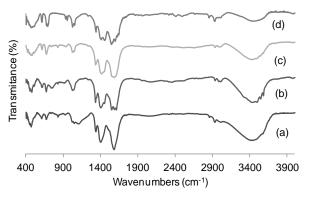

Fig. 4 DRIFT spectrum of synthesized Zn-Ac salt (a) and Zn-Ac thermally treated at: (b) 100 °C, (c) 120 °C, (d) 140 °C.

The diffractograms for the synthesized Zn-Nit and the resulting salt under different thermal treatments are shown in Figure 5. For all the samples, the characteristic peaks were located at 2θ = 9.06° (200), 34.46° (221) and 26.94° (510). The cell parameters were a=19.48 Å, b=6.25 Å and c=5.59 Å, which according to the JCPDS card N°04-011-5271 are assigned to the crystal phase of Zn$_5$(OH)$_8$(NO$_3$)$_2$.2H$_2$O, indicating the thermal stability of Zn-Nit.

The DRIFT spectra for the synthesized Zn-Nit and the resulting salt under different thermal treatments are presented in Figure 6.

For all the samples, in the region of the OH group stretching vibrations (2900-3700 cm^{-1}), the band at the lower frequency is attributed to the OH groups involved in hydrogen bonding, and the sharp band located at 3573 and 3637 cm^{-1} at the upper frequency limit is related to the free OH groups.[38,44,45,46]

The band located at 1373 cm^{-1} is assigned to the stretching mode of free nitrate ions. The other nitrate absorption bands are the weak bands located at 765 cm^{-1} and 835 cm^{-1}. The weak band at 1063 cm^{-1} is attributed to N-O stretching of free nitrate groups. The weak broad band at 1015 cm^{-1} is attributed to the O-H bending mode in the Zn-OH entities. The strong band at 1635 cm^{-1} is characteristic of the bending vibrations of the interlayer water molecules. In the sample treated at 140 °C, a new peak was present at 1498 cm^{-1}, indicating a modification in the nitrate coordination to Zn-anion.
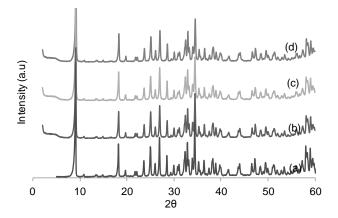

Fig. 5 X-ray diffraction pattern of synthesized Zn-Nit salt (a) and Zn-Nit thermally treated at: (b) 100 °C, (c) 120 °C, (d) 140 °C.
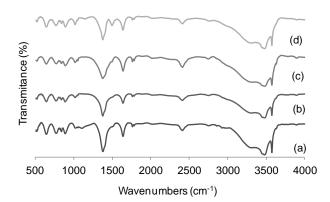

Fig. 6 DRIFT spectra of synthesized Zn-Nit salt (a) and Zn-Nit thermally treated at: (b) 100 °C, (c) 120 °C, (d) 140 °C.

The SEM images of the synthesized solid catalysts and the thermally-treated samples are shown in Figures 7 and 8. In the image corresponding to Zn-Ac (Fig. 7), the particles are flake-like, and this texture opens with increasing temperature until 120 °C, originating bigger flakes smaller in thickness. At 140 °C, the particles are more compact, with straight edges.

For Zn-Nit, the SEM image shows plate-like particles. This morphology did not change in the temperature range studied, but the size and thickness of the particles gradually decreased at 100 and 120 °C, and remained constant at 140 °C.
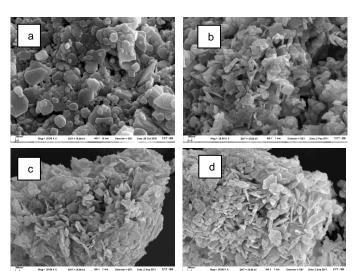
Fig. 7 SEM image of (a) synthesized Zn-Ac salt, and (b) Zn-Ac thermally treated at: (b) 100 °C, (c) 120 °C, (d) 140 °C.
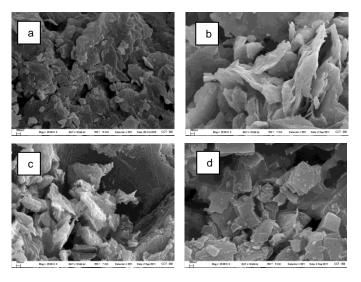

Fig. 8 SEM image of (a) synthesized Zn-Nit salt, and (b) Zn-Nit thermally treated at: (b) 100 °C, (c) 120 °C, (d) 140 °C.

3.2. Catalytic activity

3.2.1. Mass transfer resistance in the transesterification of soybean oil with methanol

In view that transesterification reaction takes place in two immiscible phases, the reaction was studied at different stirrer rates from 300 to 1100 rpm in order to quantify the impact of external mass transfer resistance on the reaction rate. These experiments (presented in Figure 9) showed that the triglyceride conversion and FAME yield were independent of the agitation rate above 500 rpm. Hence, all further experiments were conducted at a stirrer rate of 500 rpm to ensure that there was no external mass transfer resistance.
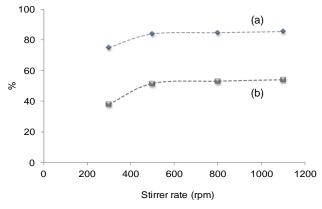

Fig. 9 Triglyceride conversion (a) and FAME yield (b) at different stirrer rates for Zn-Nit catalyst at 100 °C.

The Weisz-Prater criterion (Eq.3) was used to evaluate the intraparticle diffusion limitations for triglyceride (TG):

$$\Phi_{TG} = \frac{(-r_{obs,TG})\rho_c D_p^2}{36\, D_{eff,TG}\, C_{TG}} \qquad (3)$$

where $r_{obs,TG}$ is the observed initial TG rate [$2.0\ 10^{-5}$ mol/s kg$_{cat}$], ρ_c is the apparent density of the catalyst [kg/m^3], D_p is the particle diameter [$2.67\ 10^{-5}$ m], D_{eff} is the effective diffusion coefficient [m^3/s] and C_{GT} is the triglyceride concentration [454.3 mol/m^3]. The effective diffusivity is given by:

$$D_{eff,TG} = \frac{D_{TG,MOH}.\varepsilon}{\xi} \qquad (4)$$

The Weisz-Prater criterion indicates that the mass transfer limitation for the unknown kinetics is negligible when $\Phi_i < 0.03$-0.7.[47]

The selected value for the tortuosity factor (ξ) was 4,[48] and the porosity (ε) was calculated by:

$$\varepsilon = \rho_c \times V_{pore} \qquad (5)$$

The pore volume was 2.6×10^{-5} m^3/kg.

The triglyceride-methanol diffusion coefficient was evaluated using the Wilke and Chang correlation. As methanol is used in large excess, the diffusivity of TG in methanol was considered and calculated by the following expression[49]:

$$D_{TG,MeOH} = 7.4 \times 10^{-8} \frac{\sqrt{\Phi_{MeOH} M_{MeOH}}}{\eta_{MeOH}\, v_{TG}^{0.6}} T \qquad (6)$$

where $D_{TG,MeOH}$ is the diffusion coefficient of TG in methanol (cm^2/s), Φ_{MeOH} is the association factor of methanol (1.9), M $_{MeOH}$ is the molecular weight of methanol (32 g/mol), T is temperature (373 K), η $_{MeOH}$ is the viscosity of methanol (0.218 cP), and vTG is the molar volume of TG at 100 °C (957 cm^3/mol).

The molecular diffusivity of TG in methanol was $D_{TG} = 1.6 \times 10^{-9}$ m^2/s.

In the present experiments, the numerical value of the Weisz-Prater module was 8.4×10^{-5} for TG, indicating that it is possible to neglect the concentration gradients within the catalyst particle.

Catalysis Science & Technology Accepted Manuscript

The Weisz-Prater module was calculated for TG because it is the reactant of the largest size and it is present in a lower concentration.

3.2.2. Transesterification of soybean oil with methanol

The results of triglyceride conversion and FAME yield at final reaction time are presented in Table 2. At 100 °C, a conversion of 94.4% and 83.9% was observed for Zn-Ac and Zn-Nit, respectively, with a FAME yield of 63.1% and 51.5%. When the samples were studied at 140 °C, conversions were close to 99% with yields of 81.7 and 76.8% for Zn-Ac and Zn-Nit, respectively.

The differences in activity shown by the catalysts at 100 °C (Table 2) are explained by the characterization results.

The diffractogram for the spent catalyst is shown in Figure 10. Zn-Ac shows identical XRD patterns used at 100 and 140 °C, and they are different from that corresponding to the original sample. The XRD patterns indicated that the crystalline structure corresponded to zinc glycerolate (2θ= 10.9, 20.75 and 17.2°).

Table 2 Transesterification of soybean oil with methanol: triglyceride conversion (%), FAME yields (%), reaction time: 120 min.

Reaction temperature	100 °C		140 °C	
Catalyst	Conversion	Yield	Conversion	Yield
Zn-Ac	94.4	63.1	99.7	81.7
Zn-Nit	83.9	51.5	98.6	76.8

For Zn-Nit at 100 °C, the diffraction pattern of the spent catalyst (Fig.10.c) corresponds to the original crystalline structure (2θ = 9.20, 18.35 and 27.08°). For Zn-Nit at 140 °C (Fig.10.d), the XRD pattern corresponds to zinc glycerolate.
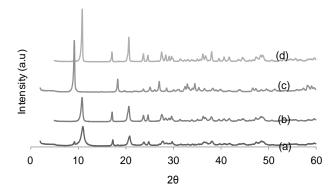

Fig. 10 X-ray diffraction pattern of (a) Zn-Ac (T$_{RX}$=100 °C), (b) Zn-Ac (T$_{RX}$=140 °C), (c) Zn-Nit (T$_{RX}$=100 °C), (d) Zn-Nit (T$_{RX}$=140 °C).

Figure 11 presents the DRIFT spectra of Zn-Ac after reaction at 100 °C (Fig.11.a) and 140 °C (Fig.11.b). The spectra present the characteristic strong bands of glycerol at 2700-2400, 2050-1900 and 1500-1350 cm^{-1}.[50] As indicated in the experimental section, the samples used were washed extensively with THF/methanol, and therefore the bands observed in the IR of the solid correspond to zinc glycerolate and not to the presence of glycerol adsorbed on the solid (this was corroborated by the XRD analysis of the sample).

Fig. 11.c presents the DRIFT spectrum of Zn-Nit after reaction at 100 °C. The spectrum is characteristic of the synthesized salt, as

shown in Fig. 6.a. For Zn-Nit after reaction at 140 °C, the spectrum presented the characteristic vibration band of Zn glycerolate.
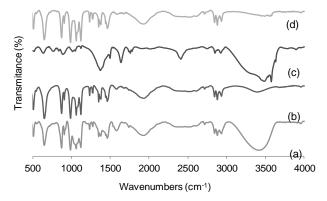

Fig. 11 DRIFT spectra of (a) Zn-Ac (T$_{RX}$=100 °C), (b) Zn-Ac (T$_{RX}$=140 °C), (c) Zn-Nit (T$_{RX}$=100 °C), (d) Zn-Nit (T$_{RX}$=140 °C).

Summarizing the above results, Zn-Nit remained stable in the reaction medium at 100 °C, whereas Zn-Ac at 100 °C and both solids at 140 °C transformed into zinc glycerolate in the reaction medium. These results explain for the similarities in TG conversions and FAME yield presented in Table 2 for Zn-Ac at 100 °C and both Zn-Nit and Zn-Ac at 140 °C.

Zinc glycerolate was studied as a new catalyst for an environmentally friendly production of biodiesel.[56] The solid showed a long life and could be reused without deactivation or selectivity loss.

Figure 12 shows the evolution of the products and reactants over time for the Zn-Nit catalyst at the temperature at which the solid was stable (100 °C). The typical behavior of a reaction in series can be observed, where the concentration of TG drops to form DG, which reach their maximum at 40 min of reaction. On the other hand, ever increasing values of MG and FAME concentrations were found for the studied reaction time.

This behavior is different from that reported by Zieba et al.[30] for triacetin transesterification at 50 °C, who observed that the content of diacetin reached a plateau after a short reaction time. After the plateau, the content of diacetin virtually did not decrease. Very low amounts of monoacetin and FAME were observed only when the conversion of triacetin was relatively high (50-60%). The authors proposed that the "plateau" reached by partial glycerides in the presence of Zn-Nit catalyst could be ascribed to the accumulation of glycerol/partial glycerides on the catalyst surface as the result of strong interactions of glycerides with alkaline centers of Zn-5 catalyst.

The results presented in this work demonstrate that the effect of catalyst poisoning by adsorption can be reverted with a temperature increase (within the stability range of the catalyst), enabling the desorption of the species adsorbed on the catalyst surface, and their subsequent reaction.

The activity of Zn-Nit (with weak basic sites) was good compared to other catalyst with similar basicity. The solid ZnO (with weak basic sites) was not active at 65°C, [51] and it showed a 80% FAME yield after 24 h with 12.5 wt% catalyst at 120°C. [52] It was also reported a 77.5% FAME yield at 200°C after 4 h of reaction in the transesterification of crude coconut oil. [53]

The solid Zn-Nit can be also compared with ZrO$_2$ with weak acid and base sites on the surface. [54,55] The solid ZrO2 presented (at 200°C) 31% TG conversion and 8.4% of FAME yield in the

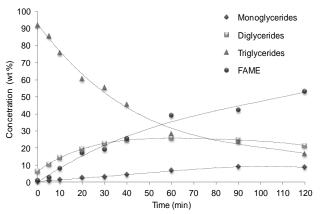sunflower oil transesterification[54] and 49.3% FAME yield for crude coconut oil.[53]

Fig. 12 Evolution of products and reactants over time for the Zn-Nit catalyst at 100 °C.

Fig. 13 XRD pattern of used Zn-Nit catalyst after (a) two and (b) three reaction cycles in the transesterification of soybean oil at 100 °C.

Fig. 14 SEM image of spent Zn-Nit salt after three reaction uses at 100 °C.

3.4. Study of the catalysts in consecutive uses in the transesterification of soybean oil
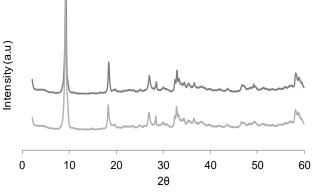
Zn-Nit was studied in three consecutive transesterification reactions at 100 °C. The results, presented in Table 3, show that there were no important changes in the activity of the catalyst along the cycle of reuses. The triglyceride conversion and FAME yield remained constant, as well as the product distribution. Again, it is notable the high FAME selectivity presented by this catalyst.
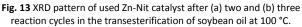
The X-ray diffraction patterns of the catalyst used in reaction (Figure 13) were in agreement with those of the original solids (Figure 5.a), without significant changes in the cell parameters (a= 19.43 Å, b= 6.27 Å, and c= 5.46 Å) and the apparent size of the crystal (9.7 Å and 9.6 Å after two and three reaction cycles). These results were confirmed by infrared spectroscopy (not shown). Catalyst morphology also remained constant after three uses (Fig. 14).

After each catalytic test, the catalyst was centrifuged, washed and weighed. The theoretical content of zinc in the Zn-Nit sample was 51.98 wt.%, and the experimental value determined by AAS was 51.23 wt.%. The polar and non polar phases were recovered from reaction medium and the zinc content was analyzed. Zn was not detected in neither of the liquid phases recovered by AAS.

Table 3 Reusability of the Zn-Nit catalyst in the transesterification of soybean oil with methanol at 100 °C.

Catalytic test	1	2	3
TG Conversion (%)	83.9	83.6	83.6
FAME Yield (%)	51.5	52.1	52.8
FAME Selectivity (%)	61.4	62.4	63.2
MG (%)	8.6	9.8	9.2
DG (%)	21.5	19.3	19.1
TG (%)	16.5	16.9	16.9
FAME (%)	53.3	54.0	54.8

In view of the high level of activity obtained for Zn-Nit at 140 °C, its reuse was studied, despite knowing that it would transform into Zn glycerolate. The results on TG conversion an FAME yield are presented in Table 4, showing a decrease of 10% in conversion and of 20% in yield.

The high activity shown in its first use could be attributed to the presence of a number of sites available for the reaction: Brønsted base sites of the hydroxy salt (it undergoes degradation during reaction) and of the zinc glycerolate.[56,57] In the second and third uses, the amount of catalyst was 3% (zinc glycerolate).

3.5. Effects of water on the transesterification of soybean oil

The effect of water content on the transesterification reaction was investigated by adding 0.5 wt% of water (with respect to oil) into the reaction medium under usual conditions. The results are shown in Table 5. For comparison, the resulting reaction under the same conditions without water (using methanol HPLC grade) is also presented.

In the presence of water oil conversion and FAME yield decreased to 61.5 and 29.2%, respectively. The product distribution (Table 5, 2 h reaction time) showed that FAME and MG concentrations were low in catalytic tests with 0.5% of water, and final concentration of DG and TG were higher in the presence of water. In view of these observations, it can be suggested that some species are adsorbed on the catalytic surface, preventing the reaction from proceeding.

Table 4 Reusability of the Zn-Nit catalyst in the transesterification of soybean oil with methanol at 140 °C (reaction time: 2 h): triglyceride conversion and FAME yield.

Catalytic test	1	2	3
TG Conversion (%)	98.6	91.2	92.8
FAME Yield (%)	76.8	59.2	58.3
FAME Selectivity (%)	77.8	65.0	62.9
MG (%)	8.6	10.8	12.7
DG (%)	7.6	18.3	19.3
TG (%)	1.4	9.1	7.5
FAME (%)	82.4	61.7	60.5

Fig. 15 Evolution of products and reactants in the transesterification of soybean oil/0.5% water with methanol at 100 °C.

The evolution of reactants and products in the transesterification with 0.5% water is presented in Fig.15. The concentration of TG fell slowly to a value of 38.8% at 120 min, and the MG, DG and FAME fraction increased over the time range analyzed.

Even though the reaction was slower than in absence of water (Fig.12), at the same TG conversion the product distribution was similar for both catalytic tests. For example, for a TG conversion of ~44%, the product concentration in the reaction without water (t_{rx}=30 min) was DG=22.6%, MG=3% and FAME=19.1%. In the presence of water (t_{rx}=60 min) the concentration was DG=22.6%, MG=3.3% and FAME=17.2%.

The XRD pattern of the spent Zn-Nit catalyst is shown in Fig. 16, and it reveals that the solid remained unchanged (without any significant change in the basal spacing: 9.7 Å).

The final acidity value was 1.7 (mg KOH/g). In a previous work,[57] Zn-Ac and Zn-Nit were used in the oleic acid esterification reaction. Experimental results indicated that nitrate and acetate ions could have been replaced with the oleate ion in the layered material. In the present study, however, the acidity present was not enough to modify the solid.

Fig. 16 XRD pattern of the spent Zn-Nit catalyst in the transesterification of soybean oil with 0.5 wt.% water, at 100 °C.

Table 5 Transesterification of soybean oil with methanol using Zn-Nit as catalyst at 100 °C (reaction time: 2 h): product distribution, triglyceride conversion and FAME yield.

Composition of the non-polar phase (wt.%)	Water content	
	0 wt.%	0.5 wt.%
MG	8.6	5.6
DG	21.5	26.0
TG	16.5	38.8
FAME	53.3	29.6
Fatty acids	-	-
TG conversion (%)	83.9	61.5
FAME yield (%)	51.5	29.2
Acidity* (mg KOH/g)	1.8	1.7

*determined by titration of a sample representative of the reaction media (both phases)
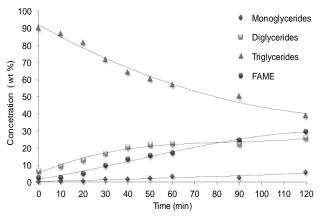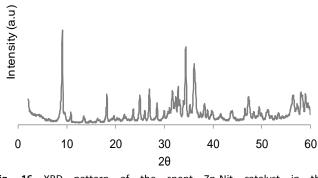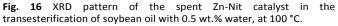
Conclusions

The zinc hydroxy acetate salt (Zn-Ac) and zinc hydroxy nitrate (Zn-Nit) were prepared, and their correct synthesis was confirmed by X-ray diffraction and FTIR spectrometry. These solids were evaluated in the transesterification of soybean oil with methanol, in absence of external or internal mass transfer limitations.

Zn-Nit was tested in the transesterification of soybean oil at 100 °C for 2 h, and it showed a 83.9% oil conversion with a 51.5% FAME yield. This catalyst showed a long life and could be reused for several catalytic cycles without deactivation, even when the solid presented water loss from its molecules. Zn-Nit showed good tolerance to water, and the catalyst remained unchanged. Zn-Ac was not stable, and at 100 °C the salt transformed into Zn glycerolate in the reaction medium.

Acknowledgements

Notes and references

Planta Piloto de Ingeniería Química PLAPIQUI (UNS – CONICET), Camino "La Carrindanga" Km 7, CC 717, CP 8000, Bahía Blanca, Argentina. FAX: 54-291-4861600; e-mail: gtonetto@plapiqui.edu.ar

1 C. Drapcho, J. Nghiem and T. Walker, Biofuels Engineering Process Technology., New York: McGraw-Hill; 2008.

2 A. Srivastava and R. Prasad, Energ. Rev. 2000, **4**, 111-133.

3 D. López, J. Goodwin Jr., D. Bruce and E. Lotero, *Appl. Catal. A*, 2005, **295**, 97–105.

4 M. Kouzu, T. Kasuno, M. Tajika, Y. Sugimoto, S. Yamanaka and J. Hidaka, *Fuel*, 2008, **87**, 2798–2806.

5 X. Liu, H. He, Y. Wang and S. Zhu, *Catal. Comm.*, 2007, **8**, 1107–1111.

6 H. Mootabadi, B. Salamatinia, S. Bhatia and A. Abdullah, *Fuel*, 2010, **89**, 1818–1825.

7 G. Tonetto and J. Marchetti, *Top. Catal.*, 2010, **53**, 755-762.

8 M. Di Serio, M. Ledda, M. Cozzolino, G. Minutillo, R. Tesser and E. Santacesaria, *Ind. Eng. Chem. Res.*, 2006, **45**, 3009-3014.

9 O. Babajide, N. Musyoka, L. Petrik and F. Ameer, *Catal. Today*, 2012, 190, 54-60.

10 W. Xie, H. Peng and L. Chen, *J. Mol. Catal. A: Chem.*, 2006, **246**, 24-32.

11 Y. Liu, E. Lotero, J. Goodwin and X. Mo, *Appl. Catal. A*, 2007, 331,138-148.

12 H. Zeng, Z. Feng, X. Deng and Y. Li, *Fuel*, 2008, **87**, 3071‑3076.

13 J. Shumaker, C. Crofcheck, S. Tackett, E. Santillan-Jimenez, T. Morgan, Y. Ji, M. Crocker and T. Toops, *Appl. Catal. B,* 2008, **82**, 120–130.

14 E. Li, Z. Xu and V. Rudolph, *Appl. Catal. B*, 2009, **88**, 42‑49.

15 G. Suppes, M. Dasari, E. Doskocil, P. Mankidy and M. Goff, *Appl. Catal. A*, 2004, **257**, 213-223.

16 Y. Xie and R. Davis*, J. Catal*., 2008, **254**, 109-197.

17 M. Di Serio, R. Tesser, M. Dimiccoli, F. Cammarota, M. Nastasi and E. Santacesaria, *J. Mol. Catal. A: Chem.*, 2005, **239**, 111–115.

18 S. Chin, A. Almad, A. Mohamed and S. Bhatia, *Appl. Catal. A*, 2006, **297**, 8-17.

19 M. Di Serio, R. Tesser, L. Pengmei and E. Santacesaria, *Energy Fuels*, 2008, **22**, 207-217.

20 S. Yan, H. Lu and B. Liang, *Energy Fuels*, 2008, **22**, 646-651.

21 W. Xie and X. Huang, *Catal. Letters*, 2006, **107**, 53–59.

22 Z. Yang and W. Xie, *Fuel Process. Technol.*, 2007, **88**, 631-638.

23 Y. Taufiq-Yap, H. Lee, M. Hussein and R. Yunus, *Biomass Bioenergy*, 2011, **35**, 827-834.

24 Z. Kesić, I. Lukić, D. Brkić, J. Rogan, M. Zdujić, H. Liu and D. Skala, *Appl. Catal. A*, 2012, **427-428**, 58-65.

25 K. Tanabe, K. Shimazu, H. Hattori and K. Shimazu, *J. Catal.*, 1979, **57**, 35-40.

26 P. Rossi, G. Busca, V. Lorenzelli, M. Waquif, O. Saur and J. Lavalley, *Langmuir*, 1991, **7**, 2677-2681.

27 W. Jiang, H. Lu, T. Qi, S. Yan and B. Liang, *Biotechnol. Adv.*, 2010, **28**, 620-627.

28 T. Montanari, M. Sisani, M. Nocchetti, R. Vivani, M. Herrera Delgado, D. Ramis, G. Busca and U. Costantino, *Catal. Today*, 2010, **152**, 104-109.

29 C. Cordeiro, G. Carabajal Arizaga, L. Pereira Ramos and F. Wypych, *Catal. Comm.*, 2008, **9**, 2140-2143.

30 A. Zieba, A. Pacula and A. Drelinkiewicz, *Energy Fuels*, 2010, **24**, 634-645.

31 D. Reinoso, M. Fernandez, D. Damiani and G. Tonetto, *Int. J. Low Carbon Tech.*, 2012, **7**, 348-356.

32 A. Zieba, A. Pacula, E Serwicka and A. Drelinkiewicz, *Fuel*, 2010, **89**, 1961-1972.

33 J. Auffredic and D. Louer, *J. Solid State Chem.*, 1983, **46**, 245-252.

34 T. Biswick, W. Jones, A. Pacula, E. Serwicka and J. Podobinski, *J. Solid State Sci.*, 2009, **11**, 330-335.

35 L. Poul, N. Jouini and F. Fievet, *Chem. Mater*. 2000, **12**, 3123-3132.

36 E. Hosono, S. Fujihara, T. Kimura and H. Imai, *J. Colloid Interface Sci.*, 2004, **272**, 391-398.

37 E. Kandare and J. Heossenlopp, *J. Phys. Chem. B.*, 2005, **109**, 8469-8475

38 S. Newman and W. Jones, *J. Solid State Chem.*, 1999, **148**, 26-40.

39 K. Tanabe, M. Misono, Y. Ono and H. Hattori, New solid acid and bases. Their catalytic properties, Studies in surfaces science and catalysis. Elsevier: Amsterdan, 1989.

40 F. Vanlaar, D. De Vos, F. Pierard, A. Mesmaeke, L. Fiermans and P. Jacobs, *J. Catal.*, 2001, **197**, 139-150.

41 T. Biswick, W. Jones, A. Pacuła, E. Serwicka and J. Podobiński, *J. Solid State Chem.*, 2007, **180**, 1171-1179.

42 C. Lin and Y. Li, *Mat. Chem. Phys*. 2009, **113**, 334–337.

43 V. Koleva and D. Stoilova*, J. Mol. Struc,* 2002, **611**, 1-8.

44 C. Chouillet, J. Kraft, C. Louis and H. Lauron-Pernot, *Spectrochim. Acta Part A*, 2004, **60**, 505-511.

45 F. Wypych, G. Carbajal Arízaga and J. Ferreira da Costa Gardolinski, *J. Coll. Interf. Sci*. 2005, 283, 130–138.

46 M. Hussein, M. Ghotbi, A. Yahaya and M. Rahman, *Sol. Stat. Sci*. 2009, **11**, 368–375.

47 K. Westerterp, W. Van Swaaij and A. Beenackers, Chemical reactor design and operation. John Wiley & Sons: New York, 1987.

48 H. Fogler and L. Scott, Elements of chemical reaction engineering, 3rd ed., Prentice Hall: New Jersey, 1999.

49 J. Portha, F. Allain, V. Coupard, A. Dandeu, E. Girot, E. Schaer and L. Falk, *Chem. Eng J.*, 2012, **207-208**, 285-298.

50 H. Dong and C. Feldmann, *J. Alloys Comp.*, 2012, **513**, 125-129.

51 Z. Yang and W. Xie, *Fuel Proces. Tech*., 2007, **88**, 631–638.

52 S. Dasari, M. Doskocil, E. Mankidy and P. Goff, *Appl Catal A*, 2004, **257**, 213-223.

53 J. Jitputti, B. Kitiyanan, P. Rangsunvigit, K. Bunyakiat, L. Attanatho, and P. Jenvanit-panjakul, Chem. Eng. J., 2006, **116**, 61–66.

54 H. Sun, Y. Ding, J. Duan, Q. Zhang, Z. Wang, H. Lou and X. Zheng, *Bioresource Tech.*, 2010, **101**, 953-958.

55 R. Silva Rodrigo, J. Hernandez Enrıquez, A. Castillo Mares, A. Melo Banda, R. Garcıa Alamilla, M. Picquart and T. Lopez Goerne, *Catal. Today*, 2005, **107-108**, 838-843.

56 D. Reinoso, D. Damiani and G. Tonetto, *Appl. Catal. B*, 2014, **144**, 308-316.

57. D. Reinoso, D. Damiani and G. Tonetto, *Appl. Catal. A*, 2012, **449**, 88-95.